Real-time moment analysis of pulmonary nitrogen washout

JAFAR SANIIE, GERALD M. SAIDEL, AND EDWARD H. CHESTER
Departments of Biomedical Engineering and Medicine, Case Western Reserve University and Veterans Administration Medical Center, Cleveland, Ohio 44106

SANIIE, JAFAR, GERALD M. SAIDEL, AND EDWARD H. CHESTER. *Real-time moment analysis of pulmonary nitrogen washout.* J. Appl. Physiol.: Respirat. Environ. Exercise Physiol. 46(6): 1184–1190, 1979.—A real-time moment analysis was applied to multibreath nitrogen-washout dynamics of the lung. Because the analysis accounts for breathing pattern variations, subjects could perform the washout with spontaneous breathing. The real-time digital processing of the nitrogen and flow signals incorporates filtering, delay compensation, and corrections for the effects of gas composition and temperature changes. In our study, moment analysis of the multibreath washout was evaluated for 37 subjects: 6 normal nonsmokers, 4 "normal" smokers, 6 asthmatics, 12 with diffuse interstitial disease, and 9 with chronic obstructive pulmonary disease. Moments were computed from end-tidal and breath-averaged nitrogen fractions. The ratio of 1st-to-0th moments was found to yield distinctions among subjects with different degrees of ventilation inhomogeneity, even between normal nonsmokers and "normal" smokers. With minimal computational facilities, this moment analysis not only provides a sensitive index of ventilatory dysfunction, but also a cost-effective tool.

ventilation inhomogeneity; multibreath washout; spontaneous breathing; computer analysis; smokers

WITH THE AVAILABILITY of digital computation facilities in pulmonary function laboratories, more sophisticated data processing and analyses can be used to yield better differentiation of mild as well as severe pulmonary dysfunction. In particular, function tests such as the multibreath lung washout can be made feasible for routine clinical evaluation of ventilation inhomogeneity as well as functional residual capacity. Although many indices of ventilation inhomogeneity based on multibreath nitrogen-washout dynamics have been proposed, Saidel et al. (11) and Fleming et al. (4) reported that moment ratios give superior quantitative distinction among subjects with mild-to-severe ventilation inhomogeneity. (The ratio of 1st-to-0th moments is the mean; from the mean and 2nd-to-0th moments, the variance can be defined.) The ratio of 1st-to-0th moments of the washout curve, formed by the sequence of end-tidal N_2 fractions, are related to the nonuniform alveolar flow-volume distribution (12).

Inasmuch as moments are computed from all the points of the washout curve, they include more information and are affected less by measurement error than other indices computed from relatively few points (1, 3, 9, 14). Models with a specified structure (5, 6–8, 10) can also be used to characterize the entire washout curve, but these demand a parameter estimation procedure that typically requires an optimization algorithm. In addition, the computation of model parameters is significantly more costly than the computation of moments. For clinical purposes, real-time evaluation of moments can be easily managed by use of a simple minicomputer or even a microprocessor.

To investigate the effectiveness of moment analysis in quantifying ventilation inhomogeneity, we studied subjects with normal function and those with various pulmonary diseases. We compared the moment ratios for two different truncation points of the washout data. Several types of moment ratios were compared with respect to reproducibility and discrimination.

EXPERIMENTAL METHODS

Clinical subjects. We studied 37 subjects who represented five separate categories: *1*) normal nonsmoker with no history of chronic or recurrent lung disease, respiratory symptoms, or history of smoking; *2*) "normal" smoker with no history of chronic or recurrent lung disease, respiratory symptoms, but a history of cigarette smoking greater than 5 pack-yr; *3*) diffuse interstitial lung disease (DILD) with diffuse chronic inflammatory disease of lung parenchyma (e.g., interstitial fibrosis); *4*) bronchial asthma with episodic wheezing and dyspnea with intervals free of clinical symptoms; and *5*) chronic obstructive pulmonary disease (COPD), which is not asthmatic, with persistent chronic obstruction to airflow (e.g., emphysema and/or bronchitis).

Pulmonary function was assessed in all subjects by spirometry, dilution lung volumes, and body plethysmography (Table 1). In addition, steady-state carbon monoxide diffusing capacity (D_{LCO}) was evaluated. There were six normal nonsmoking subjects and four "normal" smokers who averaged 15 pack-yr of cigarette smoking each and were normal by all these pulmonary functions tests. The six asthmatic patients were all asymptomatic, but five of them had reduced forced expiratory flow rates from 25 to 75% of the total forced vital capacity ($FEF_{25-75\%}$). Four of the six also had increased specific airway resistance (SRaw) in the body plethysmograph, and three were hyperinflated. All six had a normal diffusing capacity. Only one was normal by all parameters tested and therefore in a true remission, i.e., no detectable physio-

TABLE 1. *Pulmonary function studies*

	n	$FEF_{25-75\%}$, l/s	FRC, liters	TLC, liters	SRaw, cmH_2O/s	D_{LCO}, ml/min·Torr
Normal nonsmokers	6	4.4 ±0.9	3.0 ±0.9	6.2 ±1.4	4.1 ±1.0	26 ±10
"Normal" smokers	4	4.7 ±1.2	2.9 ±0.8	5.6 ±1.5	4.0 ±1.1	21 ±5
Asthmatics	6	1.8 ±1.4	3.1 ±1.1	6.0 ±1.6	12.3 ±9.1	19 ±5
DILD	12	2.4 ±1.3	1.9 ±0.5	4.3 ±0.8	5.4 ±3.2	11 ±6
COPD	9	0.3 ±0.1	4.4 ±1.3	6.1 ±1.2	25.5 ±10.1	11 ±2

Values are means ± SD; n, no. of subjects. See text for abbreviations.

logical abnormalities at that time. Obviously, such a patient would still have evidence of bronchial hyperreactivity to bronchial provocation testing with methacholine. Twelve subjects had a histologically verified diffuse interstitial lung disease, seven with sarcoidosis and five with diffuse interstitial fibrosis. Ten of these 12 subjects had classical restrictive patterns manifested by reductions in total lung capacity, and seven of the 12 had decreased D_{LCO}. In addition, eight of the 12 had reduced $FEF_{25-75\%}$ and five had increased SRaw. Classical extreme patterns of ventilation inhomogeneity were shown in nine patients with chronic obstructive pulmonary disease, all of whom had moderate-to-severe obstructive ventilatory patterns and eight of nine had decreased D_{LCO}.

Testing procedure and apparatus. Subjects are tested in the following manner: in a relaxed, spontaneous fashion, the subject inhales and exhales through a pneumotachometer open to ambient air. After he becomes adjusted to the situation, he inhales fully to the total lung capacity (TLC), exhales slowly as much gas as possible to the residual volume (RV) of the lung, and returns to spontaneous breathing about functional residual capacity (FRC). Then, at the end of a quiet expiration, a valve is turned so that the inhaled gas switched from ambient air to humidified oxygen. This starts the nitrogen washout procedure which continues over a number of breaths until the end-tidal N_2 fraction is less than 2% or when 100 breaths are completed.

The gas at the airway opening is drawn continuously (3 ml/s) through a nitrogen analyzer (Med-Science Electronics model 505). The heated screen pneumotachometer is coupled to a differential pressure transducer (Validyne model MP45), the output of which is amplified and demodulated (Validyne model CD19). Both the nitrogen and flow signals are recorded continuously on FM tape for storage or put directly into analog-to-digital converters for on-line digital computation. The nitrogen and integrated flow signals are monitored simultaneously on a strip-chart recorder.

MOMENT ANALYSIS

The washout data are analyzed in terms of moments. Such data can be expressed as the normalized end-tidal N_2 fractions of each breath k

$$Y(k) = F(k)/F(0); \qquad k = 0, 1, 2, \cdots$$

where $F(k)$ is the end-tidal (peak) N_2 fraction of breath k. The independent variable of the washout curve, breath number, must be suitably scaled to minimize the effects of breathing pattern variation and lung volume (operating point). An appropriate independent variable is the dilution number, which is defined as the ratio of cumulative expired volume (CEV) to FRC as described by Saidel et al. (11). In terms of the time-varying volume flow rate $Q(t)$ integrated over expirations $E(j)$ for $j = 1, 2, \ldots, k$, the dilution number at the end of any breath k is

$$\eta_k = \sum_{j=1}^{k} \int_{E(j)} Q(t)dt/FRC$$

Qualitatively, the ratio CEV/FRC indicates the number of volume turnovers or the number of times the resting lung volume (FRC) has been diluted with an equal amount of inspired gas.

We defined the rth moment, μ_r, of the end-tidal N_2 fractions with respect to the dilution number as

$$\mu_r = \sum_{k=0}^{N} \eta_k^r \, Y(k) \, [\eta_k - \eta_{k-1}]; \qquad r = 0, 1, 2, \cdots$$

where N is chosen to be sufficiently large that no significant information is lost, i.e., $Y(N) \ll 1$. As a practical limitation, the signal-to-noise ratio can also lead to error for large N. Moments higher than the second need not be computed, because most of the information in the unimodal washout curve is contained in the first few moments. Furthermore, higher moments are more subject to the poor signal-to-noise ratio in the tail region of the washout curve.

Moments computed from the mixed-expired N_2 fraction of successive breaths can also be used to characterize the N_2 washout dynamics. Consequently, we define these moments as

$$\langle \mu \rangle_r = \sum_{k=0}^{N} \eta_k^r \, \langle Y(k) \rangle [\eta_k - \eta_{k-1}]; \qquad r = 0, 1, 2, \cdots$$

where

$$\langle Y(k) \rangle = \int_{E(k)} Y(t)Q(t)dt / \int_{E(k)} Q(t)dt$$

SIGNAL PROCESSING

The nitrogen fraction and flow (pressure difference) signals are digitized with 12-bit accuracy in real time. Samples of these signals taken at 40 Hz are processed and retained in memory only long enough to compensate for the time delay between the nitrogen and flow signals. Figure 1 is a functional diagram of data processing that incudes the following blocks: *1*) input: calibration factors and sampled input signals; *2*) signal conditioning: filtering, delay compensation, and flow correction; *3*) variables on each breath: tidal volume, end-tidal nitrogen fraction, and average nitrogen fraction; and *4*) derived quantities: lung volumes, dilution number, and moments.

Calibration. When there are zero inputs to the nitrogen analyzer and pressure signal amplifier, outputs are recorded for a few minutes before the washout test to

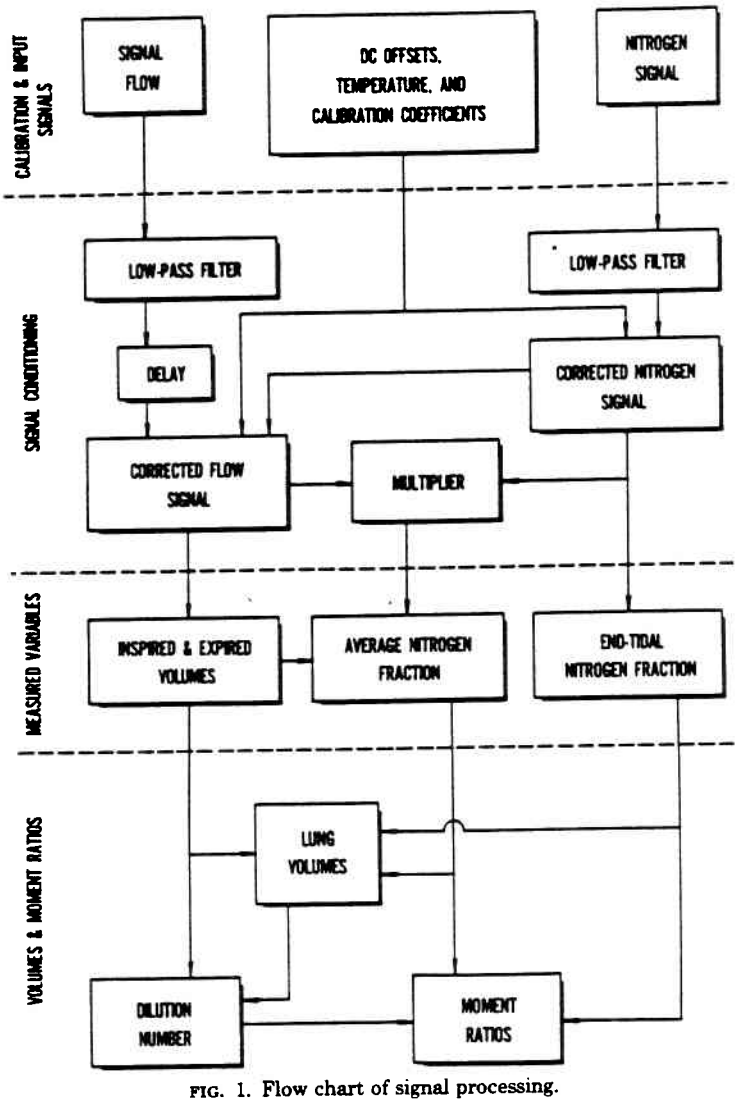

FIG. 1. Flow chart of signal processing.

llow compensation for the DC offsets. The nitrogen ignal is calibrated by assuming the N_2 fraction in the ambient air and in the lung before washout is 0.796 (dry). The flow signal is calibrated using a reciprocal pump Harvard), which provides an oscillatory flow of ambient ir through a pneumotachometer at 0.25 Hz with a cycle volume (ΔV) of 1.000 liter. The relationship between the measured pressure drop, $\Delta P(t)$, across the pneumotachmeter and the flow rate, $Q(t)$, is given by

$$Q(t) = (K/\nu)\Delta P(t)$$

here K is the volume calibration coefficient and ν is the iscosity of air at ambient temperature (e.g., $\nu = 185 \times 10^{-6}$ poise at 23°C). Integration of this equation over one-half a cycle yields

$$K = \nu \cdot \Delta V / \int \Delta P(t) dt$$

To get an accurate value of K, we calculate its mean alue from several cycles. This coefficient is the same for low in either direction. The criterion of acceptability of the K value is that its coefficient of variation be less than 1%. If this criterion is not met, it is necessary to clean and dry the pneumotachometer screen and recalibrate. The calibration factors are stored on the disk and automatically become available when they are needed in the main program.

Signal filtering. In converting flow and nitrogen signals from analog to digital form, we required an appropriate filter to improve the signal-to-noise ratio. For this purpose, we selected a second-order Butterworth low-pass filter with a cutoff frequency of 20 Hz.

Delay time compensation. The response time of the nitrogen analyzer to a sudden change in nitrogen concentration can be divided into two parts: delay time and rise time. The time delay for sampled gas to travel from the sampling valve to the ionization chamber and become ionized is approximately 75 ms. Because we use the nitrogen signal for flow signal correction and must obtain the product of nitrogen and volume flow rate at the same time, it is important that the two signals be synchronous. Consequently, we delay the flow signal also by 75 ms. Upon repeated determinations of delay time during the course of study, we found little variation (±5 ms), which is well within the digital sampling period (25 ms).

Flow-signal correction. Accurate measurement of vol-

ume flow rate at the mouth is essential for our data analysis. Consequently, we must correct the flow signal for the effects of changes in composition and temperature of the gas passing through the pneumotachometer. Differences are particularly noticeable between inspired and expired gases. The inspired gas consists of humidified oxygen at ambient temperatures; the gas leaving the mouth, however, is saturated with water at close to body temperature. Unless the screen of the pneumotachometer is heated, water vapor can condense on it to cause a change in resistance, i.e., a change in the calibration coefficient of the pressure signal.

Provided the flow is laminar, we can relate the volume flow rate $Q(t)$ and pressure difference $\Delta P(t)$ across the pneumotachometer screen by

$$Q(t) = K\frac{\Delta P(t)}{\nu(F,T)} \quad (1)$$

where the gas viscosity, ν, is a function of temperature, T, and gas composition, F = (N_2, O_2, H_2, CO_2), and K is a geometric constant. Because the mixture of gas species can be considered an ideal gas, the viscosity of the mixture can be formulated as the linear combination of viscosities of pure gas weighted by their fractional concentration F_α

$$\nu(F,T) = \sum_\alpha F_\alpha \nu_\alpha(T) \quad (2)$$

where $\alpha = N_2, O_2, H_2O, CO_2$.

The temperature changes are sufficiently small to allow the viscosities of O_2, N_2, H_2O, and CO_2 to be related linearly to temperature (2)

$$\begin{bmatrix} \nu_{N_2}(T) \\ \nu_{O_2}(T) \\ \nu_{H_2O}(T) \\ \nu_{CO_2}(T) \end{bmatrix} = \begin{bmatrix} 43.93 + 0.453T \\ 118.50 + 0.298T \\ -23.00 + 0.570T \\ 16.25 + 0.455T \end{bmatrix} 10^{-6} \text{ poise} \quad (3)$$

where T has the units of °K. The fractional concentrations (F_α) of H_2O and CO_2 in inspired gas, expired gas, and ambient air are assigned reasonable values (Table 2). Consequently, from Table 2 together with *Eqs. 1–3*, the volume flow rate at body temperature (T_b) can be computed by

$$Q(t) = K[T_b/T]\, P(t)/[A(T) - B(T)F_{N_2}(t)]$$

During inspiration, we set T = 23°C, for which A = 205.3 and B = 28.9. During expiration, we used a mean expired temperature, T = 34°C, for which A = 204.7 and B = 27.0.

TABLE 2. *Fractional concentrations of inspired and expired gas*

Species Fraction	Inspiration	Expiration	Ambient Air
F_{N_2}	$F_{N_2}(t)$	$F_{N_2}(t)$	0.790
F_{O_2}	$0.972 - F_{N_2}(t)$	$0.896 - F_{N_2}(t)$	0.200
F_{H_2O}	0.028	0.062	0.007
F_{CO_2}	0	0.041	0.003

The only directly measured fraction is $F_{N_2}(t)$. The fractional concentration of water vapor, assuming complete saturation, may be approximated by $F_{H_2O} = (13.20 - 0.61\,T + 0.04T^2)/P$, where T is temperature, in °C, and P is pressure in Torr.

Measured variables. A zero-crossing technique is applied to discriminate inspiration from expiration. Integration (by the trapezoid method) of the flow signal allows computation of maximum expiratory volume, maximum inspiratory volume, and also tidal volume during the washout test. The inspiratory and expiratory volumes over the breath k are given by

$$\Delta V(k, I) = \int_{I(k)} Q(t)dt$$

$$\Delta V(k, E) = \int_{E(k)} Q(t)dt$$

where $\Delta V(k, I)$ and $\Delta V(k, E)$ are the magnitudes of the volume changes on inspiration and expiration. The end-tidal nitrogen fraction $F(k)$ is determined by searching for the maximum point in nitrogen signal during the kth period. Multiplication of the synchronized nitrogen and flow signals leads to an estimation of averaged expired nitrogen fraction in breath k

$$\langle F\rangle_k = \int_{E(k)} F(t)Q(t)dt/\Delta V(k, E)$$

The accuracy of computer calculation of variables $F(k)$, $\langle F\rangle_k$, $\Delta V(k, I)$, and $\Delta V(k, E)$ was verified by several techniques. In particular, $F(k)$ was directly measured from the X-Y recorder. Volume amplitudes were checked with pump volumes, and the total amount of nitrogen expired over several breaths was measured from a collection bag. We found that the difference between computer and measured variables in typically ±1%.

Lung volumes. Functional residual capacity is derived from measured variables, allowing for different inspiratory and expiratory volume changes on each breath (13)

$$FRC \equiv V(0, E) = \sum_{j=1}^{k} \langle F\rangle_j \Delta V(j, E)/[F(0) - F(k)] + \sum_{j=1}^{k} [\Delta V(j, I) - \Delta V(j, E)]/[F(0)/F(k) - 1]$$

As k gets large, $F(0) \gg F(k)$ so that the second term in this equation becomes negligible. For spontaneous breathing, we make the approximations that FRC ≃ V(0, E) and at the end of expiration k the end-tidal nitrogen fraction leaving the lung is approximately equal to the N_2 fraction within the lung. In addition to the FRC, we computed the following volumes: vital capacity (VC), RV, and TLC.

EVALUATION OF INDICES

Statistical measures. In evaluating indices of ventilation inhomogeneity, we examine the sensitivity of the indices to the degree of abnormality and the variability of the indices for a given subject and among subjects in a given diagnostic group. For all indices we computed the intrasubject variability from the repeated washouts of each subject as the relative difference

$$RD = |Z_1 - Z_2|/AZ$$

where Z_1 and Z_2 are the values of any index Z for the two washouts and AZ is their average value. The diagnostic intergroup sensitivity is evaluated by the mean and standard deviation of AZ of all subjects in each group. The mathematical expressions used are presented in the APPENDIX.

Comparison of indices. Moments were computed from end-tidal and breath-averaged nitrogen fractions at a dilution number (η) of 8 or 10. From these moments, we obtained the 1st-to-0th and 2nd-to-0th moment ratios (Table 3). As previously found by Saidel et al. (11) and evaluated again in this study, the end-tidal moment ratios μ_2/μ_0 and μ_1/μ_0 at a dilution number of 10 are linearly related with a very high correlation coefficient ($\rho = 0.993$). At $\eta = 8$, these ratios are linearly related (Fig. 2) with nearly the same correlation coefficient ($\rho = 0.994$). Within any clinical group, μ_1/μ_0 tends to show less relative spread than μ_2/μ_0 at both $\eta = 8$ and $\eta = 10$. Similar results are found for the breath-averaged moment ratios ($\langle\mu\rangle_1/\langle\mu\rangle_0$ and $\langle\mu\rangle_2/\langle\mu\rangle_0$). Because the ratios involving second moments yielded no additional information, we shall not consider them further.

The remaining comparisons involve the moment ratios μ_1/μ_0 and $\langle\mu\rangle_1/\langle\mu\rangle_0$. As seen in Fig. 3, these moment ratios with $\eta = 8$ are also linearly related, having a correlation coefficient $\rho = 0.944$; with $\eta = 10$, the correlation coefficient is somewhat higher ($\rho = 0.964$). The relative variabilities among groups and subjects of these 1st-to-0th moments are also similar (Table 3). Although either of these moment ratios would be adequate for our analysis, we shall arbitrarily choose the end-tidal ratio (μ_1/μ_0) for further comparisons. We recognize that there are reasons for the use of mixed expired rather than end-tidal data to study washout dynamics. However, the end-tidal moment ratio has a clear mathematical interpretation (12). Based on a model with two alveolar spaces, one of which is poorly ventilated, the moment ratio (μ_1/μ_0) approximately equals the relative volume-flow ratio of that space. A remaining question is whether truncation of the data at dilution number $\eta = 8$ is as satisfactory as at $\eta = 10$. Although the earlier truncation of the data at $\eta = 8$ causes some loss of information, the effect on diagnostic distinction of the subjects appears to be only slightly altered (Fig. 4).

Because characteristic lung volumes and volume ratios can be determined as part of the test with very little extra effort, these also can be used to help make distinctions. In our study, the estimated FRC typically varied less than 8% for repeated tests of a given subject. The difference in the estimates of FRC with dilution 8 or 10 is even smaller than 8%. Consequently, although the FRC tends to be slightly underestimated with the smaller dilution number, the difference is not significant for comparison of among subjects. To help distinguish subjects with COPD from other diagnostic groups, we looked at the volume ratios, e.g., RV/TLC. As shown in Fig. 5, RV/TLC vs. μ_1/μ_0 tends to make this distinction clearer. No additional distinction is apparent from other lung volumes or volume ratios.

Diagnostic differentiation. With respect to normal

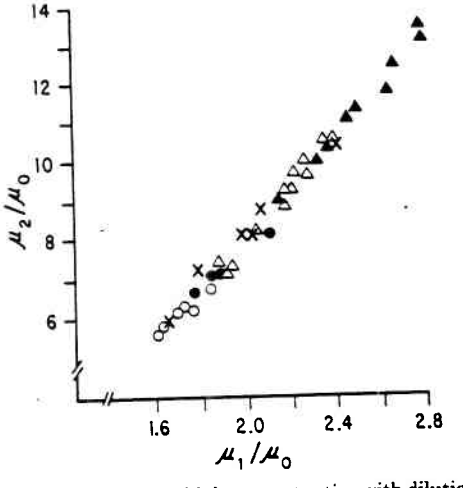

FIG. 2. Comparison of end-tidal moment ratios with dilution number of 8. Normal nonsmokers ○; "normal" smokers ●; asthma ×; DILD △; COPD ▲.

TABLE 3. *Intergroup sensitivity and intrasubject variability of moment ratios*

Diagnostic Group	Dilution No. (η)	μ_1/μ_0 Sensitivity			μ_2/μ_0 Sensitivity			$\langle\mu_1\rangle/\langle\mu_0\rangle$ Sensitivity			$\langle\mu_2\rangle/\langle\mu_0\rangle$ Sensitivity		
		MZ	SDZ	Range	MZ	SDZ	Range	MZ	SDZ	Range	MZ	SDZ	Range
Normal nonsmokers	8	1.74	0.09	1.62–1.84	6.26	0.45	5.64–7.02	1.54	0.10	1.41–1.66	5.38	0.51	4.66–5.53
	10	1.86	0.09	1.74–1.98	7.47	0.57	6.84–8.19	1.64	0.11	1.52–1.76	6.36	0.63	5.30–7.14
Normal smokers	8	1.84	0.21	1.77–2.10	6.80	1.10	7.05–8.08	1.62	0.20	1.55–1.91	5.93	1.15	5.80–7.53
	10	2.03	0.25	1.95–2.04	8.80	1.58	8.40–10.10	1.76	0.24	1.70–2.08	7.40	1.63	7.31–9.40
Asthmatic subj	8	1.97	0.26	1.79–2.40	7.92	1.44	7.18–10.35	1.68	0.18	1.44–1.94	6.42	1.20	5.60–8.18
	10	2.22	0.32	2.06–2.76	10.56	2.27	10.61–14.30	1.86	0.26	1.68–2.24	8.61	1.86	8.13–11.30
DILD subj	8	2.14	0.18	1.88–2.40	8.68	1.14	7.07–10.40	1.78	0.13	1.58–2.05	7.19	0.90	6.08–8.41
	10	2.39	0.24	2.04–2.71	11.45	1.95	8.48–14.30	2.00	0.19	1.75–2.22	9.46	1.60	7.26–11.81
COPD subj	8	2.53	0.21	2.15–2.80	11.26	1.35	8.92–13.29	2.23	0.19	1.88–2.54	9.74	1.15	7.73–11.64
	10	2.93	0.28	2.44–3.39	15.70	2.38	12.03–19.95	2.58	0.24	2.17–2.95	13.50	1.99	10.26–16.27
		Variability MRD ± SDRD%			Variability MRD ± SDRD%			Variability MRD ± SDRD%			Variability MRD ± SDRD%		
All subj	8	4.88 ± 3.60			7.29 ± 7.22			6.70 ± 5.43			10.52 ± 8.66		
	10	4.33 ± 3.09			6.53 ± 4.48			6.64 ± 6.35			9.85 ± 7.69		

Means and standard deviations for intergroup sensitivity are denoted by MZ and SDZ, where Z is one of the following indices: μ_1/μ_0, μ_2/μ_0, $\langle\mu_1\rangle/\langle\mu_0\rangle$, or $\langle\mu_2\rangle/\langle\mu_0\rangle$. Means and standard deviations for intrasubject variability are denoted by MRD and SDRD.

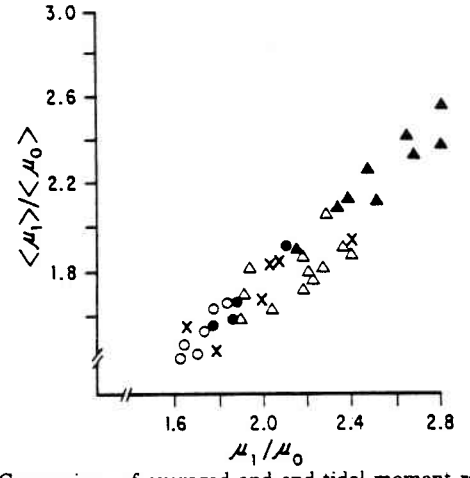

FIG. 3. Comparison of averaged and end-tidal moment ratios with dilution number of 8. Normal nonsmokers ○; "normal" smokers ●; asthma ×; DILD △; COPD ▲.

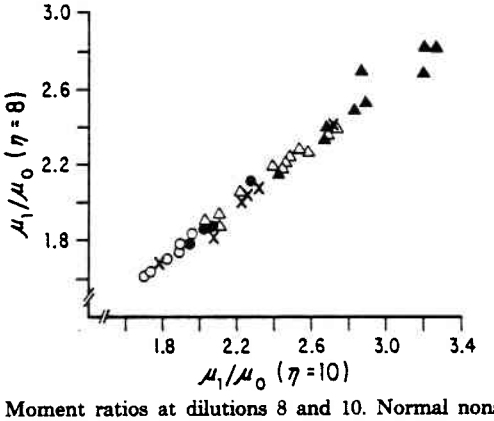

FIG. 4. Moment ratios at dilutions 8 and 10. Normal nonsmokers ○; "normal" smokers ●; asthma ×; DILD △; COPD ▲.

nonsmokers, the mean values (MZ) of μ_1/μ_0 are 9% greater for "normal" smokers, 18% greater for asthmatics, 28% greater for DILD subjects, and 57% greater for COPD subjects. By the moment ratios, abnormal subjects including the "normal" smokers are well discriminated from the normal nonsmokers. The symptomatic asthmatics have moment ratios higher than do normals; in remission, however, asthmatics have normal values for all the pulmonary function tests applied, including the indices of N_2 washout. Although the mean of μ_1/μ_0 for COPD subjects is higher than the mean for either asthmatics or DILD subjects by 39 and 29%, respectively, some asthmatics and DILD subjects have moment ratios as high as those of COPD subjects.

Although the moment ratio demonstrates differences among several clinical groups, it is not intended as a diagnostic index for a specific disease state. (Indeed, no single pulmonary function index or parameter can do that.) Rather, we use the clinical groups to give us an indication of the extent of ventilation inhomogeneity. The purpose of the moment ratio is to quantify the degree of ventilation inhomogeneity for any individual regardless of disease state.

In conclusion, with proper signal conditioning and corrections incorporated into a computerized analysis, the washout procedure can be done with spontaneous

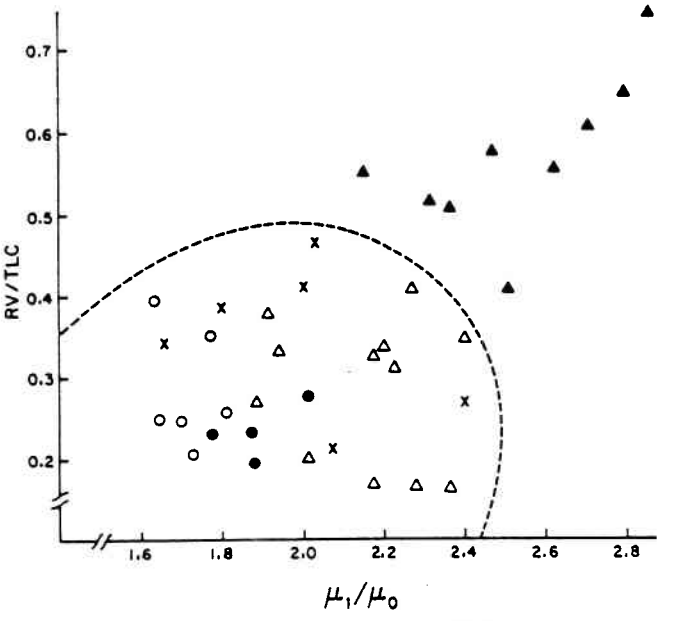

FIG. 5. Distinction of COPD subjects by RV/TLC and moment ratio with dilution number of 8. Normal nonsmokers ○; "normal" smokers ●; asthma ×; DILD △; COPD ▲.

breathing in a few minutes, even with subjects with severe COPD. By use of on-line computation, the results can be available seconds after the completion of a washout. The ratio of the 1st-to-0th moments of the end-tidal nitrogen fraction dynamics yields a quantitatively informative and clinically feasible index of ventilation inhomogeneity. This moment ratio *1*) shows little sensitivity to small measurement errors and random noise, *2*) has a relatively small range of values for normal nonsmokers, *3*) can even detect mild ventilation inhomogeneity of "normal" smokers, and *4*) can distinguish the greater inhomogeneity of subjects with asthma, diffuse interstitial lung disease, or chronic obstructive pulmonary disease.

APPENDIX

Statistical Measures

Because each subject in these experiments performed the washout procedure twice, we have two values of all indices denoted by $Z_1(I, g, s)$ and $Z_2(I, g, s)$, where I is the index, g is the diagnostic group, and s is the subject in the diagnostic group g. For each subject, we compute an average

$$AZ(I, g, s) = (Z_1 + Z_2)/2$$

and a relative difference

$$RD(I, g, s) = |Z_1 - Z_2|/AZ$$

As measures of intergroup sensitivity among diagnostic groups, we can define for each group g, having $Q(g)$ subjects, a mean

$$MZ(I, g) = \sum_{s=1}^{Q(g)} AZ(I, g, s)/Q(g)$$

and a standard deviation

$$SDZ(I, g) = \left[\sum_{s=1}^{Q(g)} [AZ - MZ]^2/Q(g)\right]^{1/2}$$

The intrasubject variability of the indices is characterized for all subjects by a mean and standard deviation of the relative difference

$$\mathrm{MRD}(I) = \sum_{g=1}^{P} \sum_{s=1}^{Q(g)} \mathrm{RD} \Big/ \sum_{g=1}^{P} Q(g)$$

$$\mathrm{SDRD}(I) = \left[\sum_{g=1}^{P} \sum_{s=1}^{Q(g)} [\mathrm{RD} - \mathrm{MRD}]^2 \Big/ \sum_{g=1}^{P} Q(g) \right]^{1/2}$$

where P is the total number of groups.

We thank Dr. Gerald M. Fleming, Lida Gamon, and Ron Lendvay for their help in data acquisition and processing.

This research was supported in part by the Medical Research Service of the Veterans Administration. J. Saniie received a summer fellowship from the Northern Ohio Lung Association.

Received 8 May 1978; accepted in final form 10 January 1979.

REFERENCES

1. BECKLAKE, M. R. A new index of the intrapulmonary mixing of inspired air. *Thorax* 7: 111–116, 1952.
2. BLUMENFELD, W., S. TURNEY, AND R. A. COWLEY. Mathematical model for flow in the heated Fleisch pneumotachometer. *Med. Biol. Eng.* 11: 546–551, 1973.
3. EDELMAN, N. H., C. MITTMAN, A. H. NORRIS, AND N. W. SHOCK. Effects of respiratory pattern on age differences in ventilation uniformity. *J. Appl. Physiol.* 24: 49–53, 1968.
4. FLEMING, G. M., J. SANIIE, E. H. CHESTER, AND G. M. SAIDEL. Sensitivity and variability of indices derived from multibreath nitrogen washout (Abstract). *Am. Rev. Respir. Dis.* 115: 106, 1977.
5. FOWLER, W. S., E. R. CORNISH, AND S. S. KETY. Lung function studies. VIII. Analysis of alveolar ventilation by pulmonary N_2 clearance curves. *J. Clin. Invest.* 31: 40–50, 1952.
6. GOMEZ, D. M., W. A. BRISCOE, AND G. CUMMING. Continuous distribution of specific tidal volume throughout the lung. *J. Appl. Physiol.* 19: 683–692, 1964.
7. LECOCQ, H. F. A theoretical analysis of the continuous distribution of specific tidal volume throughout the lung with special reference to anatomical dead space. *IEEE Trans. Biomed. Eng.* 23: 110–117, 1976.
8. PAIVA, M., AND M. DEMEESTER. Gas transport in the air phase of the lung simulated by a digital computer. *Computers Biomed. Res.* 3: 675–689, 1971.
9. PROWSE, K., AND G. CUMMING. Effects of lung volume and disease on the lung nitrogen decay curve. *J. Appl. Physiol.* 34: 23–33, 1973.
10. SAIDEL, G. M., T. C. MILITANO, AND E. H. CHESTER. Pulmonary gas transport characterization by a dynamic model. *Respir. Physiol.* 12: 305–328, 1971.
11. SAIDEL, G. M., R. B. SALMON, AND E. H. CHESTER. Moment analysis of multibreath lung washout. *J. Appl. Physiol.* 38: 328–334, 1975.
12. SAIDEL, G. M., J. SANIIE, AND E. H. CHESTER. Modeling and moments of multibreath lung washout. *Ann. Biomed. Eng.* 6: 126–137, 1978.
13. SANIIE, J. *System Identification of Ventilation Inhomogeneity by Multibreath Washout* (MS thesis). Cleveland, OH: Case Western Reserve Univ., 1977.
14. WEYGANDT, G. R. A sensitive five-breath N_2 washout test of distribution of ventilation. *J. Appl. Physiol.* 40: 464–467, 1976.